Fast-scanning near-field scanning optical microscopy using a high-frequency dithering probe

Yongho Seo and Wonho Jhe*

Center for Near-field Atom-photon Technology and School of Physics, Seoul National University, Seoul 151-742, Korea

ABSTRACT

We suggest two methods attaching tip to the quartz crystal resonator to be applied to a near-field optical scanning microscope probe. High-speed near-field scanning optical microscopy images obtained with the quartz crystal resonator probe are presented. We have achieved fast scanning imaging at the scanning speed of 1.3 mm/s without any compromise of spatial lateral resolution. Applying a concept of the acoustic wave, the topographic image of soft sample with the quartz crystal resonator probe is interpreted.

Keywords: Fast-scanning, NSOM, SNOM, AFM, Quartz, Resonator, QCR, Imaging, Acoustic, Near-field

1. INTRODUCTION

Near-field scanning optical microscopy (NSOM) [1-2] has been recently studied extensively in various fields because of its capability to obtain high resolution beyond the diffraction limit of conventional optical microscopy. In spite of its potential, slow scanning speed is one of the practical limitations to its more versatile applications. There has been extensive effort to improve the scanning speed of a scanning probe microscopy, for example, contact-mode atomic force microscopy (AFM) [3], multi probe AFM [4-5], tapping mode AFM, [6-8] and shear mode AFM. [9-10]

Though the cantilever-based AFM [3,6-7] has many advantages such as small stiffness, high force sensitivity, it can not be employed to NSOM using a tapered optical fiber as a tip, because the cantilever loaded with the heavy fiber can not vibrate. The tuning fork-based AFM / NSOM [8-9,11] has been used widely, though its scanning speed is very slow due to high Q value and low resonance frequency.

In general, the scanning speed of NSOM is limited by the dithering frequency of the tip and scanning is typically rather slow ($<10^{-2}$ mm/s). [11] The spring constant of the tuning fork is 10^3 –10^4 N/m, while that of cantilever is 10^{-1} –10 N/m. On the other hands, the Q-value of the tuning fork is 10^3 –10^4, while that of cantilever is order of 10^1 – 10^2. Low force sensitivity of the tuning fork due to its stiffness can be compromised by its high Q-value. In order to speed up the scanning speed at low dithering frequency, many ideas have been demonstrated. A frequency-detection mode using phase locked loops (PLL) was employed to solve slow settling time of the dithering amplitude [8-9] and a scanning speed of 0.23 mm/s was demonstrated by [8] with this scheme. Active Q-control modes were also developed in the tapping-mode AFM by using a ZnO_2 cantilever and a scanning speed of 2.4 mm/s was obtained.[6]

However, such AFM cantilevers are not so convenient for an NSOM, where a dithering fiber tip is typically used. Recently, Seo *et al.* [10] realized a high-frequency dithering probe by using a quartz crystal resonator (QCR), which is operated at several-MHz resonance frequency and is known to be one of the highest-frequency dithering piezo-electric devices. The spring constant of QCR is order of 10^6 - 10^7 N/m, dithering amplitude is smaller than 0.1 nm and the Q-value is 10^4 – 10^6. With this high-frequency dithering probe, a novel fast scanning shear-force microscopy [10] was demonstrated in non-contact mode. Because the QCR has a resonance frequency f_0 in the radio-frequency range (1 to 100 MHz), it is an ideal element for fast scanning purposes. Moreover, it also makes the scanning system very compact, inexpensive, and reliable with no need of lock-in amplifiers. In this paper, we report on the fastest scanning optical microscopy employing a high frequency dithering probe using QCR. We have used commercial QCRs with a resonance frequencies of $f_0 \approx 2$, 4 and 6 MHz. The diameter of the QCR is about 10 mm and its thickness is 0.8, 0.4, and 0.3 mm, respectively. As a near-field optical source and probe, a tapered optical fiber with the tip diameter of about 100 nm was used, which was produced by the conventional heating and pulling method with a CO_2 laser.

* whjhe@snu.ac.kr

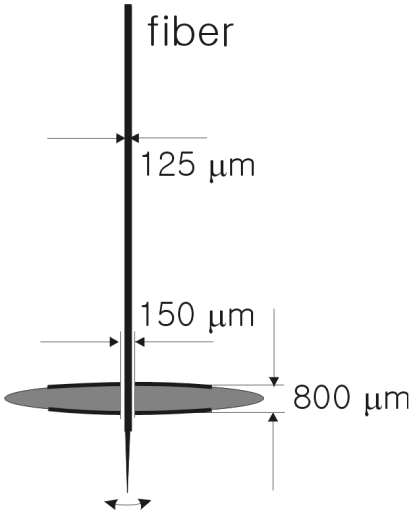

Figure 1: Perforated QCR probe.

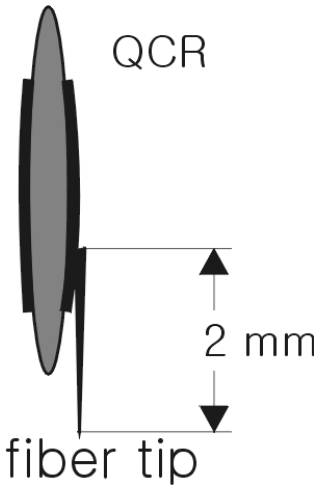

Figure 2: The QCR probe with tip attached longitudinally.

2. EXPERIMENTS

In Ref.[10], shorten tip was attached to a surface of QCR vertically. In that scheme, though high sensitive shear force signal was obtained, there was difficulty to emit or gather light at the end of the tip. Therefore, only topographic image was obtained. To be employed for NSOM, the QCR probe should be coupled to the light. We modified the QCR probe for light coupling.

2.1 perforated QCR probe

In order to allow the optical fiber to guide the light down to the fiber tip near the sample surface and also to be mechanically connected to the QCR, we perforated the QCR near its center and then inserted the tapered fiber tip into the hole, as shown in Fig.1. After several hours of careful mechanical drilling of the QCR, we can make hole. Different holes with variable diameters such as 150, 200, and 300 μm were drilled. We find that the Q-value of the QCR perforated with 300 μm hole is about 10^3, whereas that with 150 μm hole is more than 10^4. Note that the Q-value is also dependent upon the resonant frequency f_0. We used a perforated QCR that has f_0 = 2 MHz and a hole diameter of 150 μm, which showed the highest Q within our experimental methods.

The optical fiber has a cladding diameter of 125 μm, and therefore a small gap remains between the inserted fiber and the hole. We filled the gap with glue to have a rigid connection and found that the Q-value does not decrease significantly. With this fabrication scheme, we can produce high-Q QCR-based fiber probes with a high reliability, stability, and reproducibility.

Due to the thickness shear-mode operation of the QCR, the fiber tip is dithered along the lateral direction of the QCR surface as shown in Fig.1. While the dithering amplitude of QCR is about 0.1 nm, that of the tip end can be different. The resonance frequency of the fundamental mode of the tip with 1.5 mm length is about 33 kHz.[12] This value is quite different from the resonance frequency of the QCR. Therefore, the vibration of the tip is not first harmonic. That is, there are many nodes and anti-nodes in tip. The tip end should be anti-node, because it is free end, unless the tip is approached to a surface. Note that the resonance of the QCR probe is not the resonance of the tip but that including the QCR itself and the additional tip motion. As tip approaches the sample, the tip end becomes node (close end) due to shear force. Modification of the vibration mode of the tip causes frequency shift of the QCR probe.

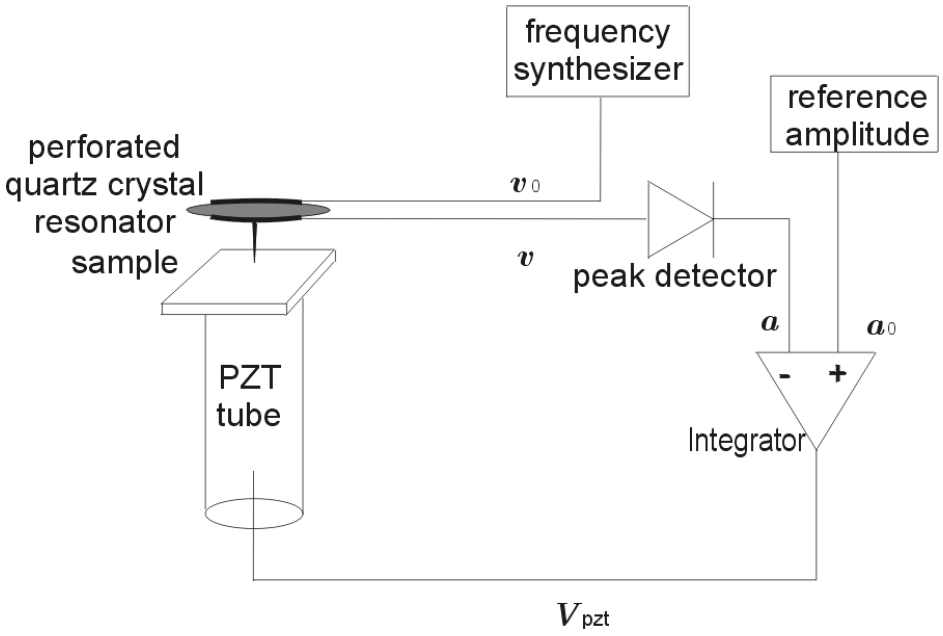

Figure 3: Amplitude detection mode feedback scheme.

2.2 longitudinal QCR probe

In order to attach a long fiber at QCR surface without mechanical manipulation, tip was attached horizontally, as shown in Fig. 2. When a tip is attached at center of the QCR, its Q value decreases seriously. Furthermore, if tip is longer than 4 mm, no change is detected when the tip approaches a surface. The tip was cut about 2 mm long, and attached at a point slightly deviated from center of the QCR with glue as shown in Fig.2. In this case, much high Q value was obtained about 10^4. This geometry has an advantage that not only the shear mode, but also tapping mode is possible, according to the angel between the tip and the dithering direction.

2.3 Scanning Scheme

In Ref.[10], the amplitude detection mode was used as shown in Fig.3. Amplitude detection mode was implemented simply, with peak detector composed into a diode and a capacitor. There were disadvantages in amplitude mode such as slow settling time and low sensitivity of the distance. Note that a critical parameter that determines the scanning speed is the decay time constant given by $\tau \cong Q / f_0$ in amplitude-detection mode operation. [9-11] In a conventional tuning-fork probe, the settling time is $5\tau > 100$ ms. Since one cannot increase the detection bandwidth much beyond the inverse of the settling time, an actuator with high f_0 and low Q is generally necessary to achieve a high scanning speed. However, a high Q-value is also essential for high-sensitivity force detection. In case of the perforated QCR, the settling time is about 10 ms and this is short enough for our purpose. Note that when a fiber tip was cut short and glued on the bottom of the QCR to be used as an AFM tip, Q was 10^3 and τ was 1 ms.[10].

A constant ac voltage v_0 from a frequency synthesizer is applied to the QCR electrode and a signal voltage v induced on the other electrode is converted into amplitude a. This signal is sent to an integrator that has an offset-reference voltage a_0. The integration time-constant (or response time) is set to 45 μs, which is 100 times longer than the oscillation period of QCR (0.5 μs). With this shear-force feedback scheme,[10] the NSOM can be operated in a non-contact scanning mode. Note that since we use only simple electronic components without a lock-in amplifier, our feedback loop is greatly simplified and its feedback bandwidth is much increased.

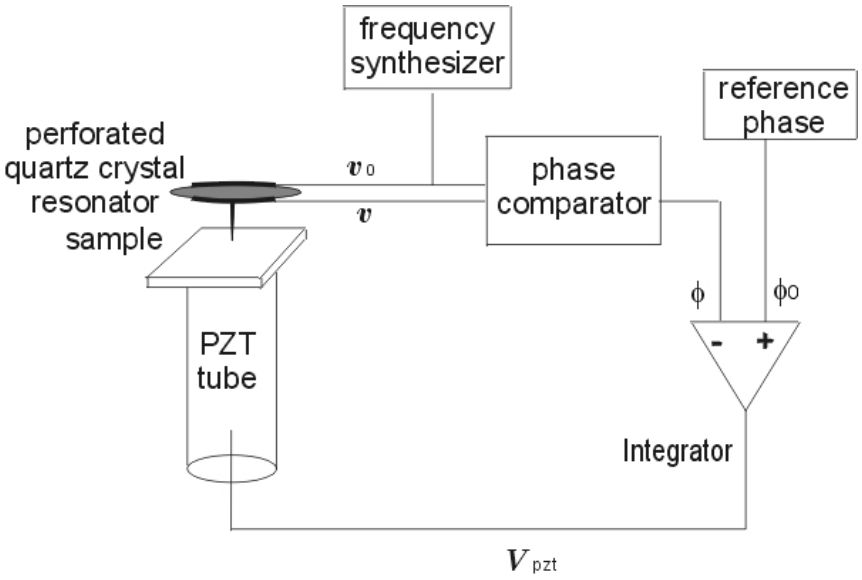

Figure 4: Feedback scheme of phase detection mode.

In case of horizontally attached tip, to increase the bandwidth of feedback loop, phase detection mode was employed. With a XOR gate, high frequency, phase mode scanning system was established. Figure 4 shows the schematic diagram of the feedback loop. The peak detector was replaced with phase detector composed into voltage comparator and XOR gate. Voltage comparator compares input voltage to a reference voltage and outputs its result as TTL signal. Through the voltage comparator, sinusoidal induced signal was changed into TTL signal and fed into XOR gate. XOR gate outputs the result of exclusive OR operation of the induced signal and reference signal from function generator. Its result is also TTL signal, become smooth through passive low pass filter. Resulting signal is proportional to the phase difference. Settling time of the phase change is faster than that of the amplitude. At resonance frequency, the phase changes more sharply than the amplitude as tip approaches a surface. More sensitive distance control was facilitated.

Figure 5 shows the experimental schematic of the reflection mode NSOM. The optical fiber with tapered tip, which is a part of a 2×1 fiber coupler, is held by the fiber chuck and inserted into the perforated QCR. One end of the coupler is coupled to the light source of laser diode operating at 660-nm wavelength and 250-mW power. The other end is placed in front of a photo-multiplier tube that detects the optical signal from the sample. The QCR is mounted on an *xyz*-translator for coarse position adjustment, whereas fine movement of the sample is controlled by a piezoelectric transducer that supports the sample stage itself.

In the Fig. 6, the approach curve of the perforated QCR probe is presented. As the tip approaches the sample, drastic reduction of the induced signal v is observed. The measured shear-force range is about 20 nm and the signal-to-noise ratio is more than 10^2 without any average process.

3. Results and Discussion

3.1 NSOM image

For a test sample, we used an optical grating that has parallel grooves with 0.8 μm pitch. Figure 7 shows the near-field optical images of the grating. In Fig. 7(a), the pixel size, the scanned area, and total scanning time is 64×64, 100 μm^2, and the 0.5 s, respectively. The scanning speed is estimated to be 1.3 mm/s, the fastest scanning speed obtained in an NSOM system. This speed is even five times faster than that of the non-contact AFM. [7] Topographic image obtained simultaneously, shows similar structures. As can be seen, all the grooves are clearly observed and well resolved in detail. Note that near the left end of the image, slight distortion of the imaged lines is found. This is associated with the limitation that the mechanical motion of the piezoelectric transducer does not follow the electrically driven positioning signal due to the very high scanning rate (128 line/s). In scanning, the sample is translated. The mass of the grating is so heavy (about 10 g), that its motion rounded at the turning point. However, its problem can be easily solved by fixing the sample and scanning the QCR probe.

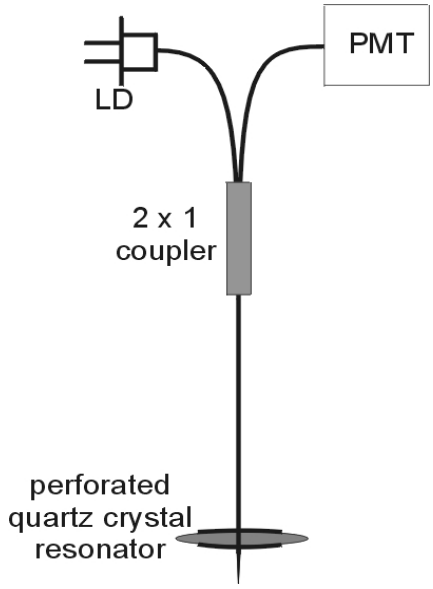

Figure 5: Near field detection scheme.

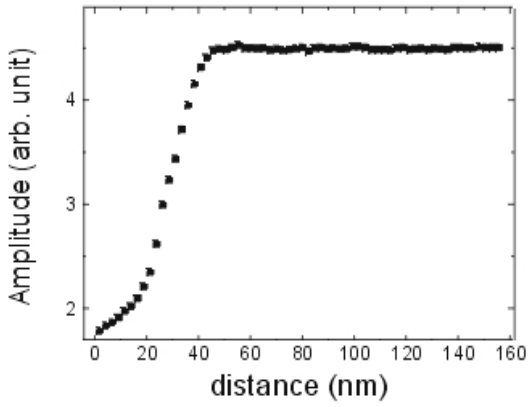

Figure 6: Approach curve of the QCR probe.

Figure 7(b) shows the similar optical image with a different scanning speed. Now, the pixel size, the total scanning time, and the scanning speed is 128×128, 1.9 s, and 0.7 mm/s, respectively. We found that a slightly better contrast for the optical image is obtained at this lower scanning speed. There, however, is not much difference with respect to the higher-speed result of Fig. 7(a) and the spatial lateral resolution for the optical images is not compromised.

We also have imaged a smaller area of 5 μm × 5 μm and 2.5 μm × 2.5 μm with the total scanning time of 0.5 s and obtained more detailed features of the grating as shown in Fig.7(c) and (d). Spatial changes in sub-micron scale is smooth which mean high signal to noise ratio. The overall spatial resolution of our fast QCR-based NSOM system is about 100 nm, which is mainly determined by the probe-tip curvature, not by the scanning speed.[10] Generally, NSOM tip is coated with metal, and the apex of the tip was milled with focused ion beam. The aperture is about < 100 nm. However, the tip used in this image is not coated with metal, so the light is not localized at the tip end, strictly.

Though QCR is very stiffer than the tuning fork, no scratch was observed in scanned surfaces, after repetitional scanning. Generally, the interaction force between the tip and sample is proportional to the spring constant of cantilever and dithering amplitude in AFM. So, the cantilever with small spring constant is desirable for soft sample. However, in case of the QCR probe, because the fiber tip is not as stiff as the QCR itself, the interaction between the tip and sample is not related to the stiffness of QCR, but the stiffness of the fiber tip. It is difficult to decide the stiffness of the fiber tip, because the vibration mode of the tip is not fundamental but several nodes and anti-nodes in the fiber tip. The interval between nodes is related to the diameter of the tip. The pulled fiber tip used in this experiment tapers, slowly and its stiffness is proportional to the diameter of the tip. The stiffness from the last node to the edge of the tip is much smaller than that of QCR. Generally, the flexural stiffness of a rod can be estimated roughly by two equations $k = m\,\omega^2$ and $k = Ewt^3/4L^3$ where m, E, w, t, L is mass, Young modulus, thickness, length of the rod, respectively. If a glass rod with 1 μm thickness has resonance frequency of 2 MHz, its length and stiffness is order of 10 μm, 10 N/m, respectively. If the average diameter of the pulled fiber tip is order of 1 μm, its stiffness ~ 10 N/m is similar to a conventional cantilever for AFM. Therefore the interacting force between the QCR probe tip and a sample is comparable to the conventional AFM, also.

3.2 Topographic images of longitudinal QCR probe

Figures 8(a) and (b) show topographic images of Al layer of a commercial compact disk (CD). CD has data pits with a stripe of which interval is 1.6 μm. The longitudinal QCR probe is used in this imaging. Its Q value was 5×10^4 and frequency was 1.998 MHz. In imaging of Fig. 8(a), an ac voltage of 1.5 V_{pp} was applied at an electrode of longitudinal QCR probe. The induced current was changed into voltage and its value is monitored with the peak detector. In this image, the data pits are clear. It took about 20 s to obtain the entire image.

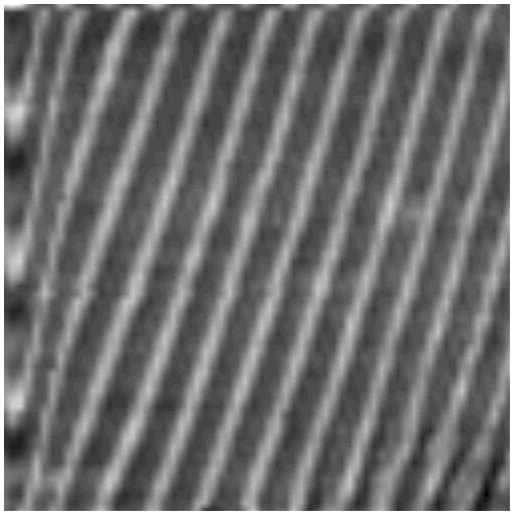

Figure 7(a): NSOM image. Total scanning time was 0.5 s. The scanned area was 10×10 mm^2.

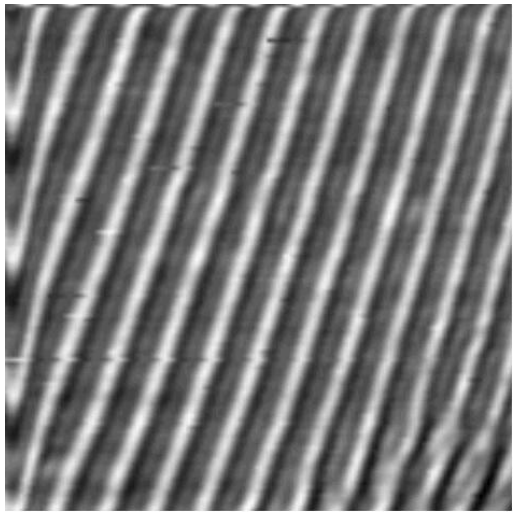

Figure 7(b): NSOM image. Total scanning time was 1.9 s. The scanned area was 10×10 mm^2.

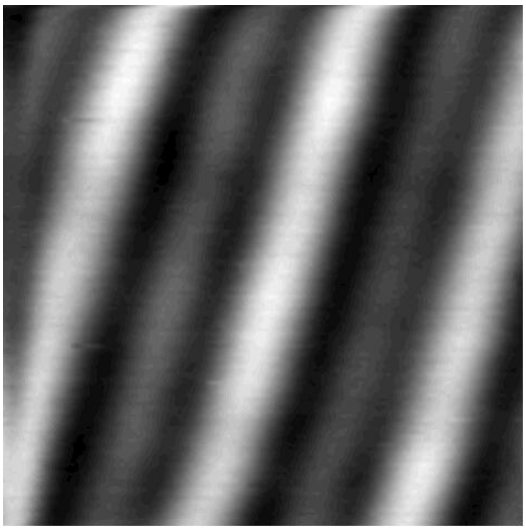

Figure 7(c): NSOM image. Total scanning time was 0.5 s. The scanned area was 5×5 mm^2.

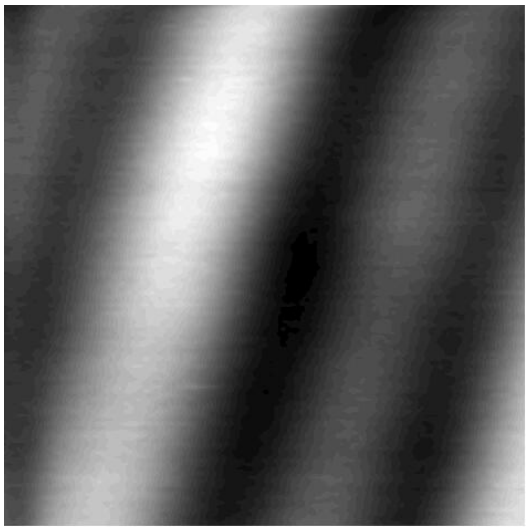

Figure 7(d): NSOM image. Total scanning time was 0.5 s. The scanned area was 2.5×2.5 mm^2.

When we compare Fig.8(a) and (b), Fig.8(b) shows more detailed image than Fig.8(a). There are irregular white dots in Fig.8(b) which are not in Fig.8(a). These dots seem to be dust, because this sample is exposed into air, for a long time. We attribute better sensitivity of Fig.8(b) to the phase detection mode. Note that the frequency dependence of phase is much larger than that of amplitude, at its resonance frequency.

In Fig. 8(b) imaging, the dithering amplitude was about 1 V_{pp}, and its induced signal is fed into the phase detector. The phase detector compares the induced signal to the applied signal. Due to its high frequency (2 MHz), the phase of reference and induced signal depends on various stray capacitance and inductance. Therefore, the phase difference at the resonance condition can be changed according to the length of the co-axial cable which transmits the electrical signals. The reference phase at the phase comparator is adjusted by changing the length of its co-axial cable between the function generator and the phase comparator. Before the tip approaches the sample, the phase difference between the reference and the induced signal is adjusted to be $\pi/2$.

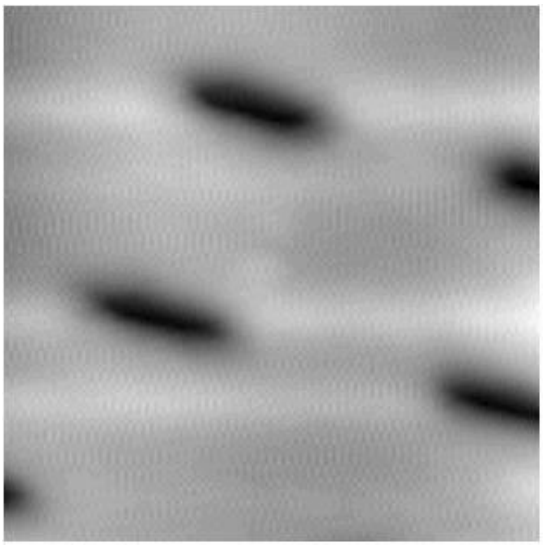

Figs. 8(a) CD image with longitudinal QCR probe. Amplitude detection mode was employed.

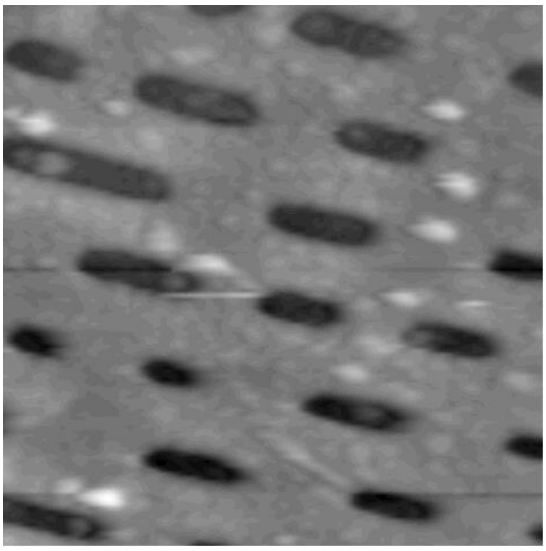

Fig. 8(b) CD image with longitudinal QCR probe. Phase detection mode was employed

While low frequency tuning fork has been employed for the NSOM probe, the high frequency QCR has been used for scanning acoustic microscopy (SAM).[13-15] The SAM is a tool for the study of the physical properties of materials and has been used for imaging interior structures and for nondestructive evaluation. In the SAM, thin film sample is coated on the QCR surface. Vibrating sample with the QCR, AFM tip scans it. As topographic image is obtained by AFM distance control, the acoustic response image is obtained through frequency shift and amplitude changes of the QCR. The acoustic response implies complicated information such as the frictional force, viscosity, and transmission of acoustic wave, *etc*.

The response of the QCR probe can be considered as a reflectance of the acoustic wave. In this picture, the tip is regarded as an acoustic wave guide line. When the tip is far from a sample, the tip end is anti-node of the acoustic wave, because it is free end. When the tip is near the sample, it becomes node (close end) and reflectance of the acoustic wave occurs. The reflectance of an acoustic wave modifies its standing wave mode. As a result, the resonance frequency of its acoustic wave is changed, and it causes the phase change. The acoustic wave is sensitive to the viscous loading. Therefore, the QCR probe suitable to a soft and viscous sample.

CONCLUSION

In summary, we suggested two methods attaching the optical fiber tip to the high-frequency QCR dithering probe to obtain near-field optical images at fast scanning speed. With the probe attached vertically, clear images of reflection mode NSOM with 1.3 mm/s scanning speed have obtained without any compromise of spatial resolution. The longitudinal QCR probe where the tip is attached at the QCR surface horizontally, facilitates troublesome gluing and supports high Q-valued resonant vibration.

We suggested a possible explanation of the QCR probe microscopy. The vibration mode of the tip is not first harmonic and the tip end is anti-node with quarter wavelength of 10 μm. The QCR probe response can be explained, applying a concept of the standing acoustic wave.

ACKNOWLEDGMENT

This work was supported by the Creative Research Initiatives of the Korean Ministry of Science and Technology.

REFERENCES

1. E. Betzig, J. K. Trautman, T. D. Harris, J. S. Weiner, and R. L. Kostelak, Science **251**, 1468 (1991).
2. E. Betzig, P. L. Finn, and J. S. Weiner, "Combined shear force and near-field scanning optical microscopy" Appl. Phys. Lett. **60**, 2484 (1992); R. Toledo-Crow, P. C. Yang, Y. Chen, and M. Vaez-Iravani, "Near-field differential scanning optical microscope with atomic force regulation" *ibid*. **60**, 2957 (1992).
3. R. C. Barrett and C. F. Quate, "High-speed, large-scale imaging with the atomic force microscope" J. Vac. Sci. Technol. B **9**, 302 (1991).
4. S. C. Minne, S. R. Manalis, and C. F. Quate, "Parallel atomic force microscopy using cantilevers with integrated piezoresistive sensors and integrated piezoelectric actuators" Appl. Phys. Lett. **67**, 3918 (1995).
5. S. C. Minne, G. Yaralioglu, S. R. Manalis, J. D. Adams, J. Zesch, A. Atalar, and C. F. Quate, "Automated parallel high-speed atomic force microscopy" Appl. Phys. Lett. **72**, 2340 (1998).
6. T. Sulchek, R. Hsieh, J. D. Adams, G. G. Yaralioglu, S. C. Minne, C. F. Quate, J. P. Cleveland, A. Atalar, and D. M. Adderton, "High-speed, large-scale imaging with the atomic force microscope" Appl. Phys. Lett. **76**, 1473 (2000).
7. N. Ookubo and S. Yumoto, "Rapid surface topography using a tapping mode atomic force microscope" Appl. Phys. Lett. **74**, 2149 (1999).
8. F. J. Giessibl, "High-speed force sensor for force microscopy and profilometry utilizing a quartz tuning fork" Appl. Phys. Lett. **73**, 3956 (1998).
9. Y. Seo, J. H. Park, J. B. Moon, and W. Jhe, "Fast-scanning shear-force microscopy using a high-frequency dithering probe" Appl. Phys. Lett. **77**, 4274 (2000).
10. W. A. Atia and C. C. Davis, "A phase-locked shear-force microscope for distance regulation in near-field optical microscopy" Appl. Phys. Lett. **70**, 405 (1997).
11. K. Karrai and R. D. Grober, "Piezoelectric tip-sample distance control for near field optical microscopes" Appl. Phys. Lett. **66**, 1842 (1995).
12. A. Drabenstedt, J. Wrachtrup and C. V. Borczyskowsky, "A distance regulation scheme for scanning near-field optical microscopy" Appl. Phys. Lett. **68**, 3497 (1996).
13. J. M. Kim ans S. M. Chang, "Scanning localized viscoelastic image using a quartz crystal resonator combined with an atomic force microscopy" Appl. Phys. Lett. **74**, 466 (1999).
14. F. Sthal ans R. Bourquin, "Characterizing mechanical resonators by means of a scanning acoustic force microscope" Appl. Phys. Lett. **77**, 1792 (2000).
15. Z. Yu and S. Boseck, "Scanning acoustic microscopy and its applications to material characterization", Rev. Mod. Phys. **67**, 863 (1995).
16. H. K. Wickramasinghe, "Contrast and imaging performance in the scanning acoustic microscope" J. Appl. Phys. **50**, 664 (1979).